

# Design and Simulation of Indigenous Roll-over Sensor for Four-Wheeler Automobiles

Piyush Raj<sup>1</sup>, Adarsh G. Datta<sup>2</sup>, Vishnu Kumar<sup>3</sup>

Centre for Nano Science and Engineering, Indian Institute of Science, Bangalore, KA, India.

## Introduction

In India, more than 150,000 people are killed each year in traffic accidents, according to the Ministry of Road Transport and Highways 2016 report. [1] This report also revealed that there have been a total of more than 450,000 accidents in the year 2016. Taking note of this, the government has tightened regulations, and from April 2019, it will be mandatory for all four wheelers to have airbags. [2] For a country which is among the largest car manufacturers in the world, this signals a stark need for making airbag sensors indigenously.

An airbag is controlled by the airbag Electronic Control Unit (ECU) which takes input from the installed sensors and actuates the deployment of the air-bag. Air-bags are required not only in case of head-on collision or high-speed braking where the sensing mechanism is rapid deceleration but also when the vehicle is skidding, which results in a rollover. In the latter case, a simple accelerometer sensor doesn't work. In such a scenario, an angular velocity sensor is required. One of the mechanisms employed for angular velocity detection is the MEMS Vibrating Gyroscope. These gyroscopes work on the principle of the Coriolis force. When the structure is vibrating in the drive direction, an angular velocity, if exists, produces motion in the sense direction which is orthogonal to the drive direction. If appropriately designed, these MEMS devices give us the required compactness and flexible functionality, as they need to be fine-tuned for different vehicle types.

Many studies have been conducted in the field of Micromachined Gyroscope technology [3] and several different mechanisms have been proposed. Out of all the mechanisms and designs, MEMS Vibrating Gyroscope stands out in terms of ease of fabrication and implementation of sensing and actuation circuitry. The simplest way of making a Vibrating MEMS Gyroscope is to use a two degree of freedom (DOF) model where a spring and damper can be thought of being attached in the drive direction and another one being attached in the sense direction. [4] However, the performance of gyroscope system with conventional 1-DOF drive and 1-DOF sense-mode oscillators is very sensitive to variations in system parameters that shift the drive or sense resonant frequencies. Under high-quality factor conditions, a high gain is achieved with a close matching of the modes, but extremely small frequency variations result in abrupt gain and phase changes. Furthermore, fluctuations in damping conditions directly affect the gain and the phases. In practical implementations, to achieve a stable response, the drive and sense mode resonant frequencies are intentionally separated. Consequently, the conventional gyroscope system that relies on the relative location of the drive and the sense resonant peaks has strict mode-matching requirements, which renders the system response very sensitive to fabrication imperfections and fluctuations in operating conditions. [5]

Since these sensors are meant for deployment in case of road accidents and in life threatening situations, mechanical robustness is a must-have requirement. Therefore, in our work, we are utilizing Multi-DOF structure, i.e., two DOF structures each in the drive

<sup>1</sup> piyushraj@iisc.ac.in

<sup>2</sup> adarshdatta@iisc.ac.in

<sup>3</sup> vishnukumar@iisc.ac.in

direction and the sense direction. This would require for us to have three mass blocks and four springs in the lumped model. Prior work by Wu et al [6] demonstrated a dual mass, fully-decoupled structure that offered high bandwidth and high linearity. However, in our case, it is not just bandwidth and linearity that needs to be within acceptable limits, but also the Angular Random Walk (ARW).

The judgment criteria, famously known as the Judgement Curve, which is a plot of angular velocity in y-axis and angle turned in the x-axis, as used by engineers at Fujitsu [7], utilizes not only the angular velocity parameter but also the angle turned by integrating the angular velocity over a period of time. This puts a severe restriction on the ARW parameter. Since, the working material

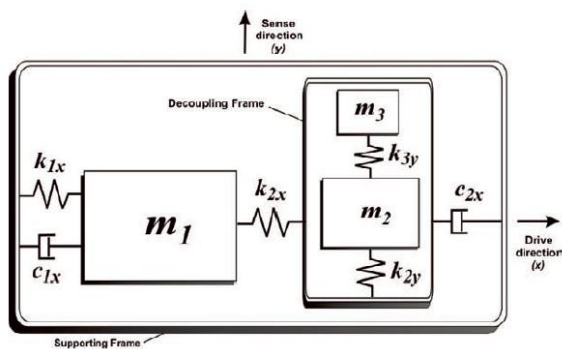


Figure 1. Spring-mass model of 4-DOF system [5]

is silicon for most MEMS device fabrication, the inherent anisotropy associated with the material makes quadrature error compensation difficult with electronic circuitry techniques. Mechanical robustness, therefore, is very much needed for the superior performance of these sensors.

In this work, we will first lay out a comparison between two-DOF structures and Multi-DOF structures on the basis of the response curve, i.e., Normalized Amplitude versus Frequency, thereby establishing the

superior performance of the latter one. We have employed interdigitated capacitance for actuation and sensing. A transimpedance amplifier is used to convert capacitance into a corresponding voltage for output detection. We then proceed to numerical simulations using replicas of the proposed structures with COMSOL Multiphysics.

## Design Objective

There are many angular velocity sensors available in the market; however, the environment in which our sensors are going to be deployed put forth some very stringent demands such as:

- 1) The vehicle, most of the time, is in a perpetual state of vibration. Therefore, the sensor needs to be mechanically robust to avoid false readings.
- 2) It needs to be compact enough to fit in the air-bag ECU.
- 3) The lifetime of these sensors needs to be more than that of the vehicle itself.
- 4) The cost should be low, and the technology used easily available in the country. Otherwise, there is no point in fabricating these indigenously.

In the lumped modeling, our structure looks like the model in Figure 1.

## Advantage of a 4-DOF structure over a 2-DOF Structure

The 2 DOF structure works in a resonance regime of the structure. This ensures high sensitivity, but it comes at a cost of low bandwidth. It is also seen that with parameter variations like damping and fabrication non-uniformity, the resonance peaks have a reduced Q-factor and shift in the frequency respectively.

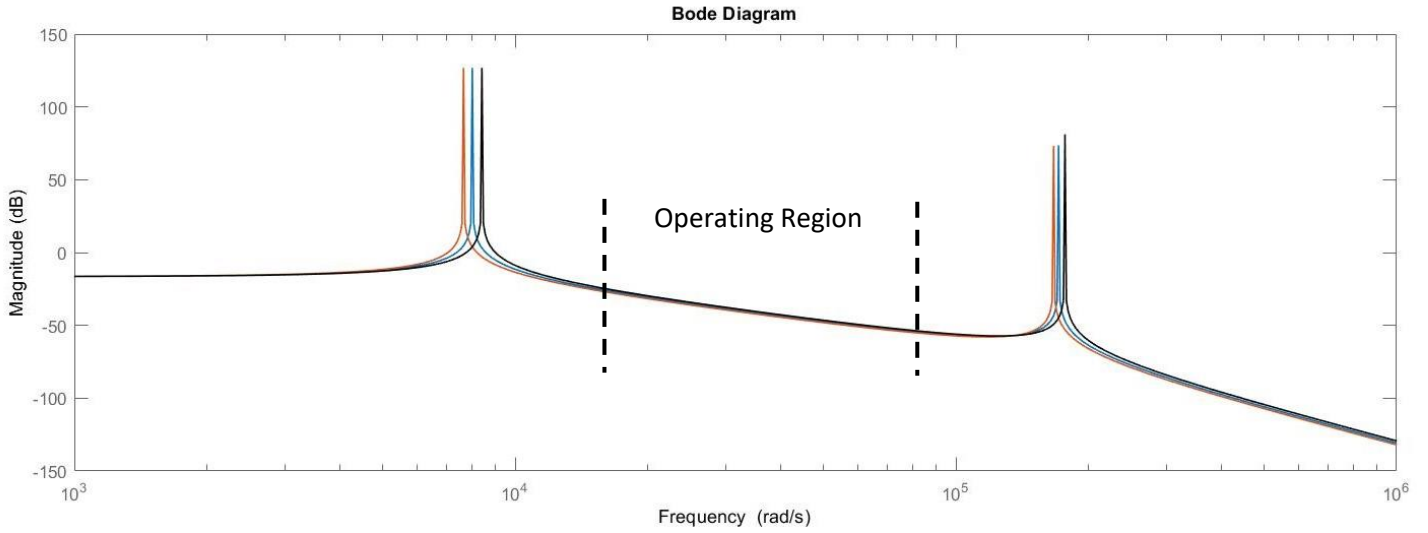


**Figure 2.** One of the uncertainty that batch fabrication brings is uncertainty in mass. Since MEMS devices have DRIE process steps, etching non-uniformity becomes an issue. The mass change causes the peaks to shift from the desired location. Conventional gyroscopes work at resonance condition and the resonance frequency shifts when mass changes, which brings about change in magnitude/displacement amplitude leading to false readings. The 4-DOF system avoids the change in displacement amplitude by operating in non-resonating condition.

In a 4 DOF system, our operating regime is in between the two resonances which gives greater operating bandwidth. This is something which is very much required as rollover time can be very small. Another advantage is that the Q-factor is very much immune to parameter variations.

### Equations governing MEMS gyroscope

The following two equations govern the drive direction:

$$m_1 \ddot{x}_1 + c_{1x} \dot{x}_1 + k_{1x} x_1 = k_{2x} (x_2 - x_1) + F_d$$

$$(m_2 + m_3) \ddot{x}_2 + c_{2x} \dot{x}_2 + k_{2x} x_2 = k_{2x} x_1$$

And the sense direction is governed by the following two equations:

$$m_2 \ddot{y}_2 + c_{2y} \dot{y}_2 + k_{2y} y_2 = k_{3y} (y_3 - y_2) + 2m_2 \Omega_z \dot{x}_2$$

$$m_3 \ddot{y}_3 + c_{3y} \dot{y}_3 + k_{3y} y_3 = k_{3y} y_2 + 2m_3 \Omega_z \dot{x}_2$$

where,  $F_d$  is the driving force and in the sense direction, we can see Coriolis

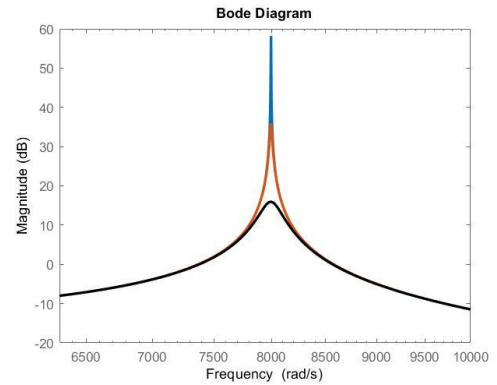


**Figure 4.** At resonance, the magnitude value changes with change in damping

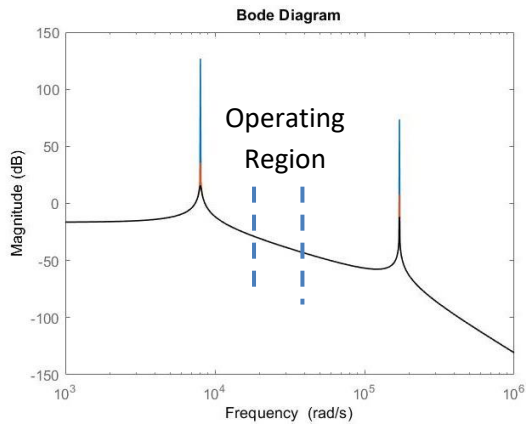


**Figure 3.** Amplitude vs. Frequency Plot for different damping coefficients. In the operating region, the Q factor hardly changes with damping values. Zoomed in part at resonance is shown in Figure 4.

force being acted in the form of  $2m_i \Omega_z \dot{x}_2$ .

We have employed variable-gap capacitive actuation, as the requirement of driving force is high in our case. Since we are working in an off-resonance condition where the Q-factor is low, the Coriolis force that eventually moves the mass in sense direction also turns out to be low if the driving force is less.

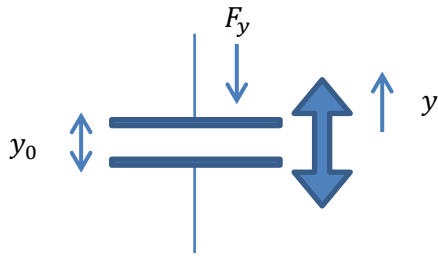


**Figure 5.** Variable gap capacitive actuator model

$$F_y = \frac{1}{2} \frac{\partial C}{\partial y} V^2 = -\frac{1}{2} \frac{\epsilon_0 z_0 x_0}{(y_0 + y)^2} V^2$$

Here, the area of the capacitor =  $(x_0 \times z_0)$  and  $V$  is the voltage. While this gives us the required force, the problem with this case is that the force varies with the square of  $V$ . In order to linearize, we put in place a balanced variable gap actuation.

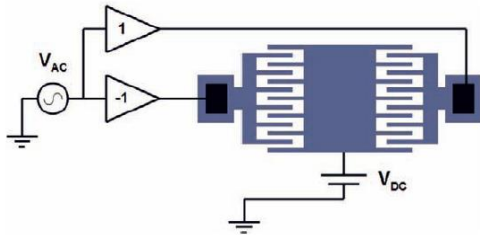


**Figure 6.** The balanced driving scheme, based on applying  $V_1 = V_{DC} + v_{AC}$  to one set of electrodes, and  $V_2 = V_{DC} - v_{AC}$  to the opposing set. [5]

$$F_y = \frac{1}{2} \frac{\partial C}{\partial x} [(V_{DC} + v_{AC})^2 + (V_{DC} - v_{AC})^2]$$

$$F_y = 2 \frac{\partial C}{\partial x} V_{DC} v_{AC}$$

$$F_{bal-pp} = 2 \frac{\epsilon_0 L t N}{d^2} V_{DC} v_{AC}$$

Here,  $L$  is the overlap length of the capacitor,  $t$  is the thickness,  $N$  is the number of interdigitated capacitor,  $d$  is the gap and  $V$  is the voltage. This linearizes the force and voltage relation.

For detection, we have used a variable gap capacitance detection mechanism where change in capacitance is given by:

$$\Delta C = \epsilon_0 \frac{tL}{d-y} - \epsilon_0 \frac{tL}{d} \approx \epsilon_0 \frac{tL}{d^2} y$$

## Design

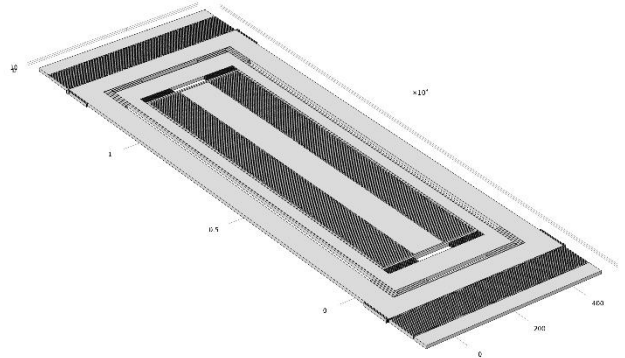


**Figure 7.** COMSOL Multiphysics design of 4-DOF MEMS Vibrating Gyroscope

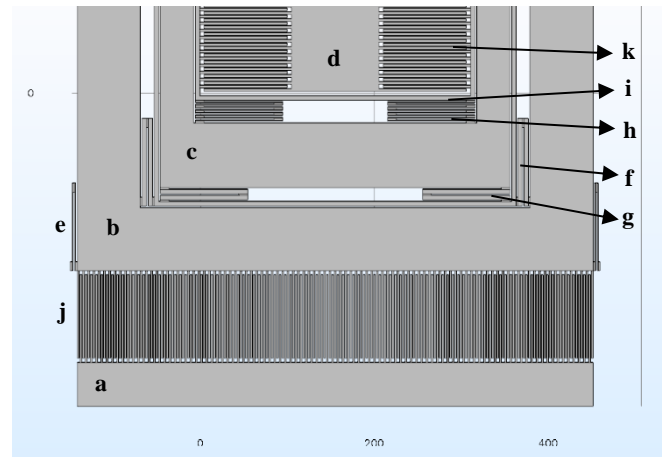


**Figure 8.** Zoomed-in picture of the device

- a = Fixed drive electrodes
- b =  $m_1$  (6.4956e-9 kg)
- c =  $m_2$  (3.41e-9 kg)
- d = Fixed sense electrodes
- e =  $k_{1x}$  (6.667 N/m)
- f =  $k_{2x}$  (714 N/m)
- g =  $k_{2y}$  (714 N/m)
- h =  $k_{3y}$  (1.66 N/m)
- i =  $m_3$  (5.087e-9 kg)
- j = Drive electrodes attached to  $m_1$  (98 × 2)
- k = Sense electrodes attached to  $m_3$  (135 × 2)

The capacitor design is common for both drive and sense with a thickness of 10 microns, an overlap length of 95 microns, a total length of 100 microns and a gap of 1 micron. They only differ in the number of electrodes. With the required data, the force generated by the variable gap capacitive actuation is  $16.48 \mu\text{N}$  considering  $V_{DC} \times v_{AC} = 0.5$ .

Finding the mass and spring constant value is tricky because they affect the placing of the resonance frequency. If they are very far away, the Q-factor at the stable operating regime is very much reduced and if they are placed very close, then the bandwidth of the operating regime is less. At the same time, the

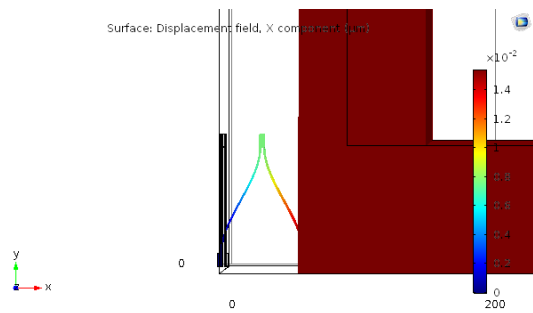


**Figure 9.** Simulation of serpentine spring. This was simulated for a constant force of  $0.1 \mu\text{N}$ .

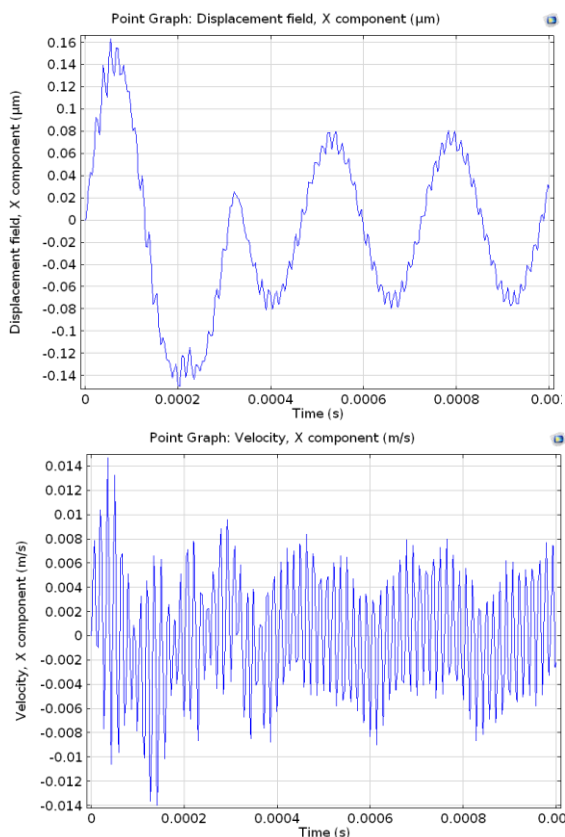


**Figure 10.** Displacement and velocity of  $m_1$  and decoupling frame respectively with sinusoidal excitation

operating region should be in between the resonance peaks of both the drive and sense modes. All these factors demand several design iterations after which we decided to drive our device at  $70 \text{ kHz}$ . We found the spring constants of the individual serpentine structures from COMSOL simulations by applying a constant force. The spring constant calculated was  $6.667 \text{ N/m}$ . Similarly, the spring constant was calculated for all the other springs that were used in the system.

The required sinusoidal driving force is  $16.48 \times \sin(4.396e5 \times t) \mu\text{N}$ . When this force was applied to the drive mass, we could extract the displacement of  $m_1$  and velocity of decoupling frame. The displacement is much less than the displacement that would cause pull-in, which usually happens at  $(1/3)^{\text{rd}}$  of the gap between the electrodes. From the velocity of the decoupling frame, Coriolis force that acts upon the sense mass is calculated by which we can get the displacement of sense mass for different angular velocity that acts on

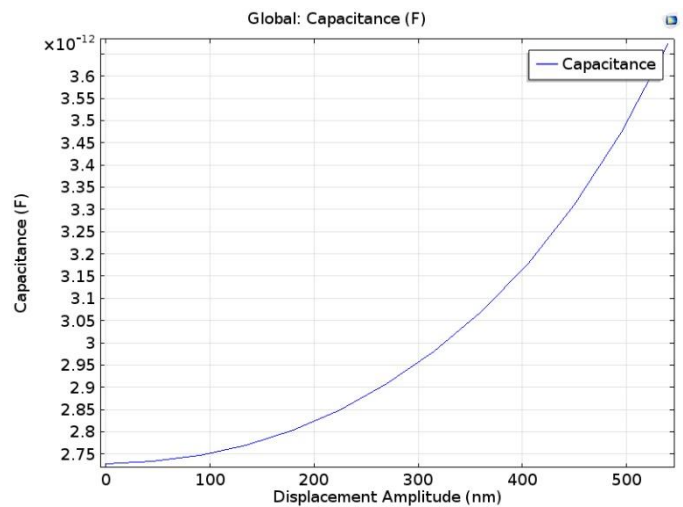


**Figure 6.** Change in capacitance with displacement of sense electrode

the system. For an angular velocity of  $1 \text{ rad/s}$ , the displacement of sense mass obtained was  $0.1 \text{ nm}$ . One of the concerns while developing an interdigitated system is the possibility of pull-in for large displacements. There is a trade-off between detectability and potentially destroying the device while detecting roll-over. In order to operate in a region where the

change in capacitance is detectable while also avoiding pull-in, we plotted the capacitance values for different displacement amplitudes of electrodes attached to  $m_3$ .

Here, zero displacement means that the sense electrodes are center aligned (exactly in the middle of the gap). We chose to place the sense electrodes at a distance of 300 nm away from the center-aligned position where the change in capacitance is significant enough and also far enough that there will be no pull-in. This ensures that the operation of device is in a more-or-less linear regime.

Since the entire geometry is computationally very intensive to simulate at

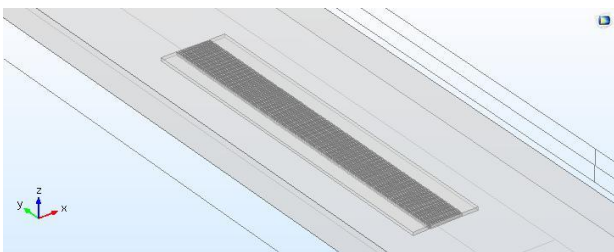


**Figure 12.** COMSOL model of the sense direction capacitor

once, we made one side of the sense direction capacitor and moved it in accordance with the different Coriolis forces being acted with different angular velocity. In the model, there are only 135 electrodes placed in Figure 12. The other half will result in only doubling the value. Since the change in capacitance is in the order of femtofarads, we will have to use on-chip detection.

## Detection

The change in capacitance due to the motion of  $m_3$  in sense direction can be detected by a change in current flowing through the sense electrode when a constant voltage is applied. This change in current could then be converted to voltage by a current-to-voltage converter. Since the change in capacitance is small, the change in current will also be proportionally small. Therefore, a gain stage is also required to boost the signal level to a detectable range. A transimpedance amplifier (TIA) built using an op-amp can accomplish

both current to voltage conversion and signal amplification. Figure 13 (a) shows a typical transimpedance amplifier implemented using an op-amp with a negative feedback resistor  $R_f$ . The output voltage of TIA is given by

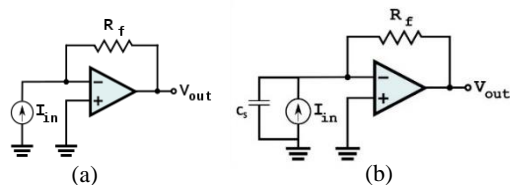


**Figure 13.** (a) A transimpedance amplifier implemented using op-amp [from Wikipedia]. (b) TIA connected to the sense electrode.  $C_s$  is modelled as the sense electrode capacitance.

$$V_{out} = -\frac{dC}{dt} (V_{bias} \times R_f)$$

In the above equation,  $V_{bias}$  is the bias applied across the sense electrodes. Thus, we directly measure the voltage proportional to the change in capacitance. This change in capacitance can be related to displacement as:

$$\frac{dC}{dt} = \frac{\epsilon A}{(d-g)^2} \frac{dg}{dt}$$

Solving this differential equation, we get

$$g = d - \frac{dC_0}{C} = d \left(1 - \frac{C_0}{C}\right)$$

In the above equation,  $d$  is the distance between the plates,  $g$  is the displacement, and  $C_0$  is the base capacitance. This distance can be converted to the force applied, which is the Coriolis force, using the same transfer function used for the lumped model. From the force, angular velocity can be calculated. But, it would be extremely difficult to implement the exact transfer function with physical elements with the desired accuracy. Thus, it is preferable to demodulate the output voltage obtained to extract the angular velocity, mathematics of which is too involved to be discussed here. To effectively extract the angular velocity, the bandwidth of the sensing system should be appropriately fixed. This

depends on the feedback resistor and other components of detection system. The sensitivity of the gyroscope depends on how much gain the detection system has. The output voltage will be in amplitude modulated form. After demodulation of the output voltage, we get an output voltage that varies in accordance with the applied angular rate. The rollover sensor detects the angular rate. The roll rate is integrated to calculate the angle (roll angle) of the car. A two-dimensional map is drawn from the roll rate and roll angle. If a

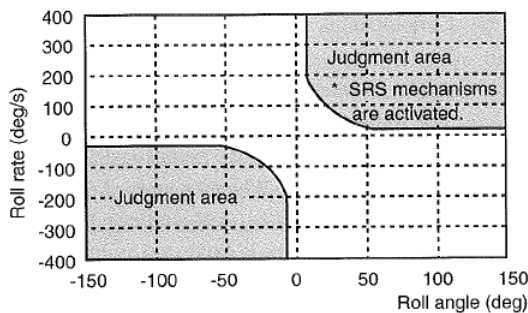


Figure 7. Judgement Curve [7]

specific judgment area is exceeded, the car is judged to have rolled over.

## Conclusion

In this work, we have established the superior performance of a 4 DOF system over a 2 DOF system with a practically feasible design. The bandwidth offered is much higher than its conventional counterpart that facilitates quick measurement which is very much needed in the event of a rollover. An on-chip detection system is required since the capacitance change is in the order of femtofarads. Finally, the angular velocity is integrated to get angular displacement and both these values are used to decide the event of the roll over.

## References

[1] Ministry of Road Transport and Highways, "Road Accidents in India - 2016," Transport Research Wing, New Delhi, 2016.

- [2] Business Standard, 05 November 2017. [Online]. Available: [http://www.business-standard.com/article/companies/airbags-speed-alerts-to-be-compulsory-by-2019-cars-to-become-costlier-117103000453\\_1.html](http://www.business-standard.com/article/companies/airbags-speed-alerts-to-be-compulsory-by-2019-cars-to-become-costlier-117103000453_1.html).
- [3] C. Y. a. L. K. Dunzhu Xia \*, "The Development of Micromachined Gyroscope Structure and Circuitry Technology," *Sensors* [www.mdpi.com/journal/sensors], no. Sensors 2014, 14, 1394-1473; doi:10.3390/s140101394, p. 80, 2014.
- [4] T. D. T. C. D. T. Nguyen Van Thang\*, "Design and Simulation of Micromachined Gyroscope Based on Finite Element Method," *VNU Journal of Science: Mathematics – Physics*, no. VNU Journal of Science: Mathematics – Physics, Vol. 33, No. 3 (2017) 77-88, 2017.
- [5] C. A. a. A. Shkel, "Structural Approaches to Improve Robustness," in *MEMS Vibrating Gyroscopes*, Springer, 2008, pp. 143-144.
- [6] G. C. Y. G. G.Q. Wu\*, "A dual-mass fully decoupled MEMS gyroscope with wide bandwidth and high linearity," *Elsevier*, no. Sensors and Actuators A 259 (2017) 50–56.
- [7] K. M. H. K. Masanori Yachi, "Development of a Roll Over Sensor," *Fujitsu Ten Tech Journal*, no. Fujitsu Ten Tech Journal, No (13), 1999.

## Acknowledgements

We would like to thank Prof. Akshay Naik and Prof. Prosenjit Sen of Centre for Nano Science and Engineering, IISc, for introducing us to the field of Micro/Nano-mechanics and guiding us with this project.